ELSEVIER

Inclusion complexes of paclitaxel and oligo(ethylenediamino) bridged bis(β-cyclodextrin)s: solubilization and antitumor activity

Yu Liu,[a,*] Guo-Song Chen,[a] Yong Chen,[a] Dong-Xu Cao,[b] Zhi-Qiang Ge[b] and Ying-Jin Yuan[b]

[a]*Department of Chemistry, State Key Laboratory of Elemento-Organic Chemistry, Nankai University, Tianjin 300071, China*
[b]*School of Chemical Engineering and Technology, Tianjin University, Tianjin 300072, China*

Abstract—The inclusion complexation behavior of paclitaxel with a series of oligo(ethylenediamino) bridged bis(β-cyclodextrin)s possessing bridge chains in different length (**1**–**4**) has been investigated in order to improve the water solubility of paclitaxel. It is found that only the long-tethered bis(β-cyclodextrin)s **1** and **2** can form the inclusion complexes with paclitaxel, which are characterized by NMR, SEM, XRD, FT-IR, TG–DTA, DSC, and microcalorimetry technology. The results obtained show that bis(β-cyclodextrin)s **1** and **2** are able to solubilize paclitaxel to high levels up to 2 and 0.9 mg/mL, respectively. The high complex stability of bis(β-cyclodextrin) **1** and paclitaxel is discussed from thermodynamic viewpoint. Furthermore, the cytotoxicity of these complexes assessed using a human erythroleukemia K562 cell line indicates that the IC$_{50}$ value of **1**/paclitaxel complex is 6.0×10^{-10} mol/dm^3 (calculated as paclitaxel molar concentration), which means that the antitumor activity of **1**/paclitaxel complex is better than that of parent paclitaxel (IC$_{50}$ value 9.8×10^{-10} mol/dm^3). This high antitumor activity, along with the satisfactory water solubility and high thermal stability of the **1**/paclitaxel complex, will be potentially useful for its clinical application as a highly effective antitumor drug.
© 2004 Elsevier Ltd. All rights reserved.

1. Introduction

Since firstly isolated from *brevifolia* as a diterpenoid natural product in 1971 by Wani et al.,[1] paclitaxel (*Taxol*®, Chart 1) has inspired further interest in developing it into a successful drug candidate due to its unique mechanism of action in promoting tubulin polymerization and stabilization of microtubules against depolymerization.[2,3] As the clinical potential of paclitaxel continues to unfold, significant advances in cancer treatment can be realized by the discovery and development of novel paclitaxel derivatives with improved efficiency, reduced toxicity, and an expanded spectrum of activity.[4–7] However, the systemic use of paclitaxel in large doses is greatly limited by not only its hematologic toxicity but also its dose dependent neurotoxicity. These limitations can be traced back to the extremely poor solubility of
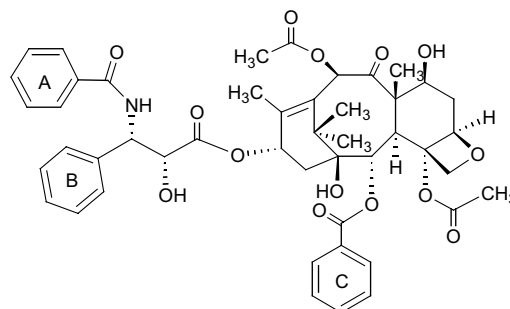

Chart 1. Structure of paclitaxel.

paclitaxel in aqueous media and its relatively high dose requirements compared to other antitumor drugs.[8] Hereto, the development of a suitable formulation of paclitaxel-based drug for parenteral administration is still extremely difficult and ultimately requires the use of a surfactant formulation containing Cremophor EL, a polyethoxylated castor oil derivative, as a major component, which inevitably leads to the side effect caused

by the introduction of Cremophor EL.[2,9] In view of these limitations of paclitaxel chemotherapy, effort including novel prodrug design maintaining antitumor activity combined with fewer side effects is imperative to allow the administration of larger doses of paclitaxel or to diminish side effects. One promising approach for a better formulation of paclitaxel is to improve the water solubility of paclitaxel by introducing some low-toxic solubilizers. Among the various inorganic and organic compounds generally used as drug carriers, cyclodextrins (CDs), a kind of truncated-cone polysaccharides mainly made up of six to eight D-glucose monomers linked by α-1,4-glucose bonds with hydrophobic interior and hydrophilic surface, are known to be able to encapsulate model substrates to form host–guest complexes or supramolecular species in aqueous solution and have been applied extensively to form inclusion complexes with all sorts of drugs in formulation and delivery systems.[10–17] However, it is demonstrated that the introduction of simple CDs only give fairly limited improvement on the solubility of paclitaxel,[18] which means that additional attempts to further increase the solubility of paclitaxel in a stable, biocompatible solvent systems are still highly sought after. Compared with natural and mono-CDs, bridged bis(β-CD)s, which possess dual hydrophobic cavities in a close vicinity and a nucleophilic or electrophilic tether with good structural variety in a single molecule, can greatly enhance the original binding ability and molecular selectivity of parent CD cavities through the potential cooperative binding of two adjacent CD units and the formation of sandwich host–guest inclusion complex.[19–21] Recently, Moser et al. reported the inclusion complexation behavior of CD dimer with paclitaxel in H₂O–DMSO solution and the biological action of the resultant CD/paclitaxel complex with human tumor cells.[22] Herein, we wish to report the preparation and cytotoxicity study of some water-soluble inclusion complexes formed by paclitaxel and bridged bis(β-CD)s (Chart 2) with different tethers. It is our special interest to explore the solubilization effect of bridged bis(β-CD)s to paclitaxel and the structure-related cytotoxicity of these inclusion complexes, which will provide a useful approach to achieving novel paclitaxel-based antitumor drug with high water solubility, high antitumor activity, and low toxicity.

2. Results and discussion

2.1. Preparation of the CD/paclitaxel inclusion complexes

In this context, we try to prepare the CD/paclitaxel inclusion complexes by the reaction of paclitaxel with bis(β-CD)s **1–4**. However, only bis(β-CD)s **1** and **2**, both of which possess a flexible long tether, are found to be able to form inclusion complexes with paclitaxel. These phenomena should be related to the structural differences among bis(β-CD)s **1–4**. For short-tethered bis(β-CD) **3**, Corey–Pauling–Koltun (CPK) molecular model study shows that the two CD cavities in **3** are too closely located in space to form a sandwich complex with paclitaxel. For Cu(II)-coordinated bis(β-CD) **4**, the coordination of copper(II) can shorten the effective length of tether group, which consequently leads to a relatively short distance between two CD cavities. Moreover, the steric hindrance from the copper(II) center located between two CD cavities is also unfavorable to the inclusion complexation of paclitaxel with CD cavities. As a simultaneous result of these two factors, Cu(II)-coordinated bis(β-CD) **4** fails to form inclusion complex with paclitaxel. With the elongation of the tether length, the two CD cavities may manage to adopt an appropriate distance and/or orientation suitable for the inclusion complexation with paclitaxel through the adjustment of flexible long tether group. Therefore, we can deduce that paclitaxel may prefer the long-tethered bis(β-CD)s upon inclusion complexation. Although the present hypothesis is drawn from a rather limited variation of bis(β-CD)s, this concept should be extended more generally to a wide variety of synthetic CD-based species and subsequently open a new channel on the design of novel formulation of paclitaxel.

2.2. Characterization of CD/paclitaxel complexes

^{1}H NMR spectra (Fig. 1) provide not only the direct evidence for the formation of CD/paclitaxel inclusion complexes but also the information about their stoichiometry. Owing to its fairly poor water solubility,[23] paclitaxel is transparent to ^{1}H NMR under most conditions when D₂O is used as solvent. Therefore, assessment of the paclitaxel complexes by ^{1}H NMR demonstrates the presence of the structural protons of the paclitaxel molecule consistent with significant solubilization. In addition, integration of the areas associated with the phenyl protons of the paclitaxel (δ 7–8 ppm) and the H-1 protons of bis(β-CD) **1** or **2** suggests a 1:2 or 1:1 inclusion complexation stoichiometry for **1**/paclitaxel or **2**/paclitaxel complex, respectively. On the other hand, Job's experiments are also performed by
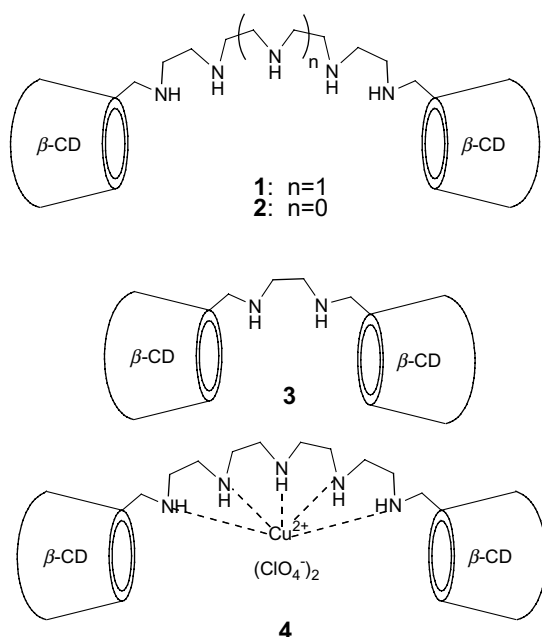

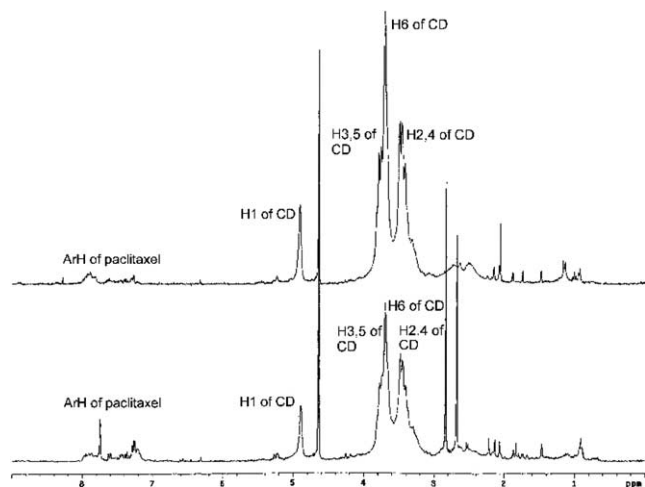
Chart 2. Structures of bis(β-CD)s **1–4**.

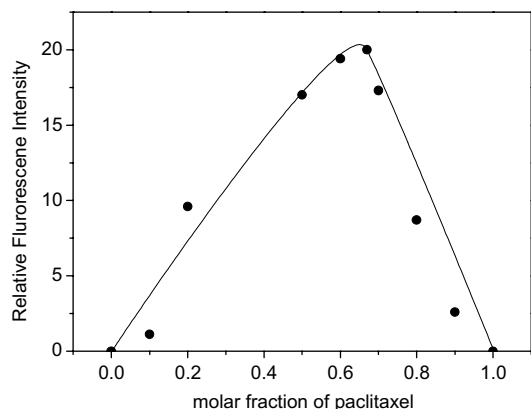**Figure 1.** ¹H NMR spectra of **1**/paclitaxel (bottom) and **2**/paclitaxel (top) complexes in D₂O at 298 K.

Figure 2. Job's plot of **1**/paclitaxel system ([bis(β-CD) **1**] + [paclitaxel] = 3.0×10^{-4} M) in a water–ethanol solution (1:1, v/v).

means of fluorescence spectroscopy to confirm this stoichiometry. Figure 2 illustrates a typical Job's plot for **1**/paclitaxel system. As can be seen in Figure 2, Job's plot of **1**/paclitaxel system shows a maximum at a molar fraction of 0.67, verifying the formation of 1:2 **1**/paclitaxel inclusion complexes. That is to say, with the longest tether group, bis(β-CD) **1** can simultaneously associate with two paclitaxel molecules to form inclusion complex, while the bis(β-CD) **2** can only bind one paclitaxel attributing to its shorter tether length. One possible explanation for this stoichiometry should be that, paclitaxel tends to form a dimer in solutions ranging from aqueous to those of low polarity through their four exchangeable hydrogen atoms (bound to heteroatoms) that can participate in inter and intramolecular hydrogen bonds.[24] Hence, there should exist the equilibrium between the paclitaxel monomer and dimer in the solution under our experimental conditions. This observation may subsequently rationalize the 1:2 and 1:1 stoichiometry for **1**/paclitaxel and **2**/paclitaxe complexes, respectively. That is, with a long linker, one bis(β-CD) **1** actually included one paclitaxel dimer in solution to form the 1:2 **1**/paclitaxel complex. On the other hand, bearing a relatively short linker as compared with **1**, one bis(β-CD) **2** can only bind one paclitaxel monomer. In addition, examinations with the Corey–Pauling–Koltun (CPK) molecular model demonstrated that a couple of paclitaxel molecules could be well accommodated in the pseudocavity formed by the long linker of bis(β-CD) **1** to form the 1:2 sandwich inclusion complex. However, for bis(β-CD) **2** with a shorter linker, the pseudocavity formed by the linker group could only accommodate one paclitaxel.

To further confirm the binding mode of bis(β-CD)s with paclitaxel, 2D NOESY experiments are completed with the spectra illustrated in Figure 3. For **1**/paclitaxel complex, it is apparent that the H-3 and H-5 protons of the
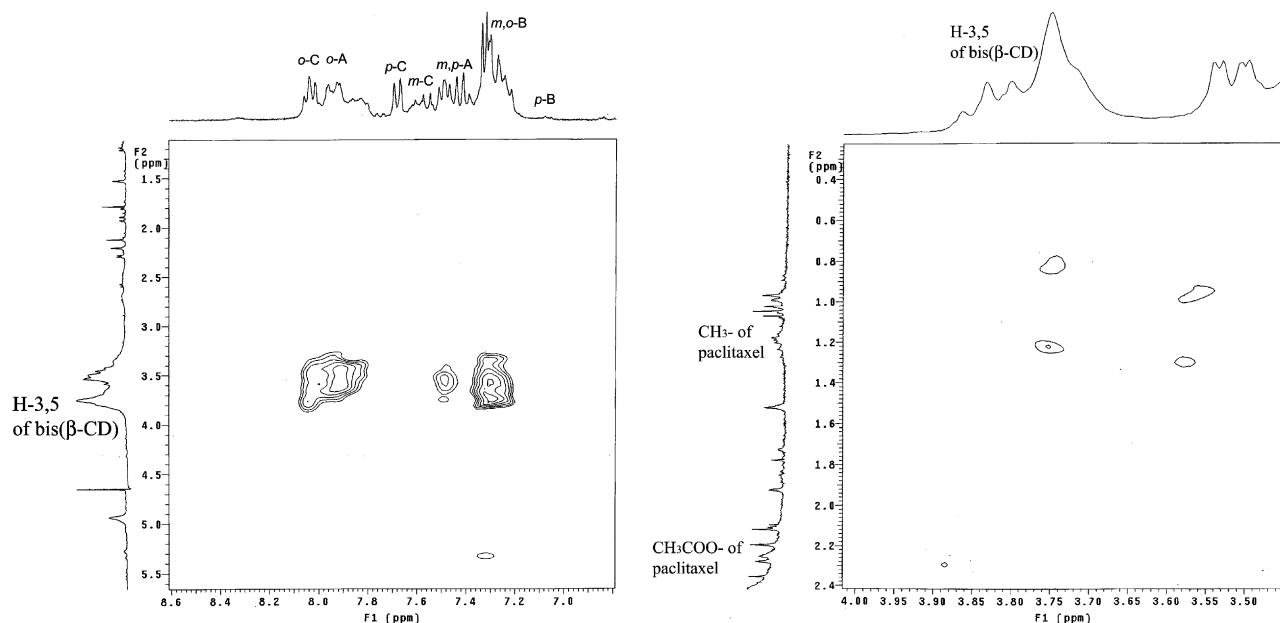

Figure 3. NOESY spectra of **1**/paclitaxel (left) and **2**/paclitaxel (right) complex in D₂O at 298 K with a mixing time of 400 ms.

CD cavities in **1** show strong correlations with the *ortho* and *meta* protons of the A and B phenyl rings and relatively weak interactions with the *ortho* protons in ring C of paclitaxel, suggesting that the CD cavities include the A and B rings in a bridging structure. A structural representation of **1**/paclitaxel complex based on the gener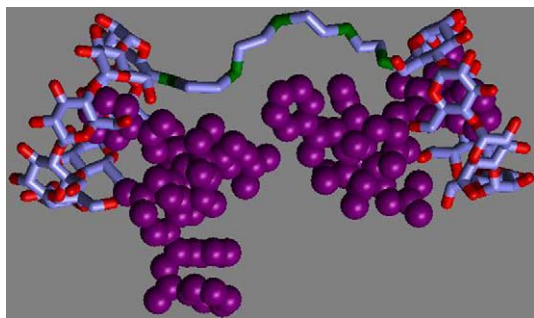ated 2D NOESY data is given in Figure 4. On the other hand, in the NOESY spectrum of **2**/paclitaxel complex, the rather weak NOE correlations between the H-3 protons of the CD cavities in **2** and the acetyl protons of paclitaxel as well as the weak correlations between H-5 protons of the CD cavities in **2** and the methyl protons in the octatomic ring of paclitaxel indicate a relatively weak association of **2**/paclitaxel complex, which inevitably results in the lower water solubility and antitumor activity of **2**/paclitaxel than those of **1**/paclitaxel complex.

In addition to the NMR data, some other experiments including scanning electron microscopy (SEM), powder X-ray diffractogram (XRD) and FT-IR also supply the evidences for the formation of CD/paclitaxel complex. The SEM images for the surface morphology of powders derived from paclitaxel, bridged bis(β-CD)s and their inclusion complexes are provided in Figure 4. A comparison of these images reveals that the apparent conformation of the complexes is distinct from that of the isolated components, those being the unmanipulated
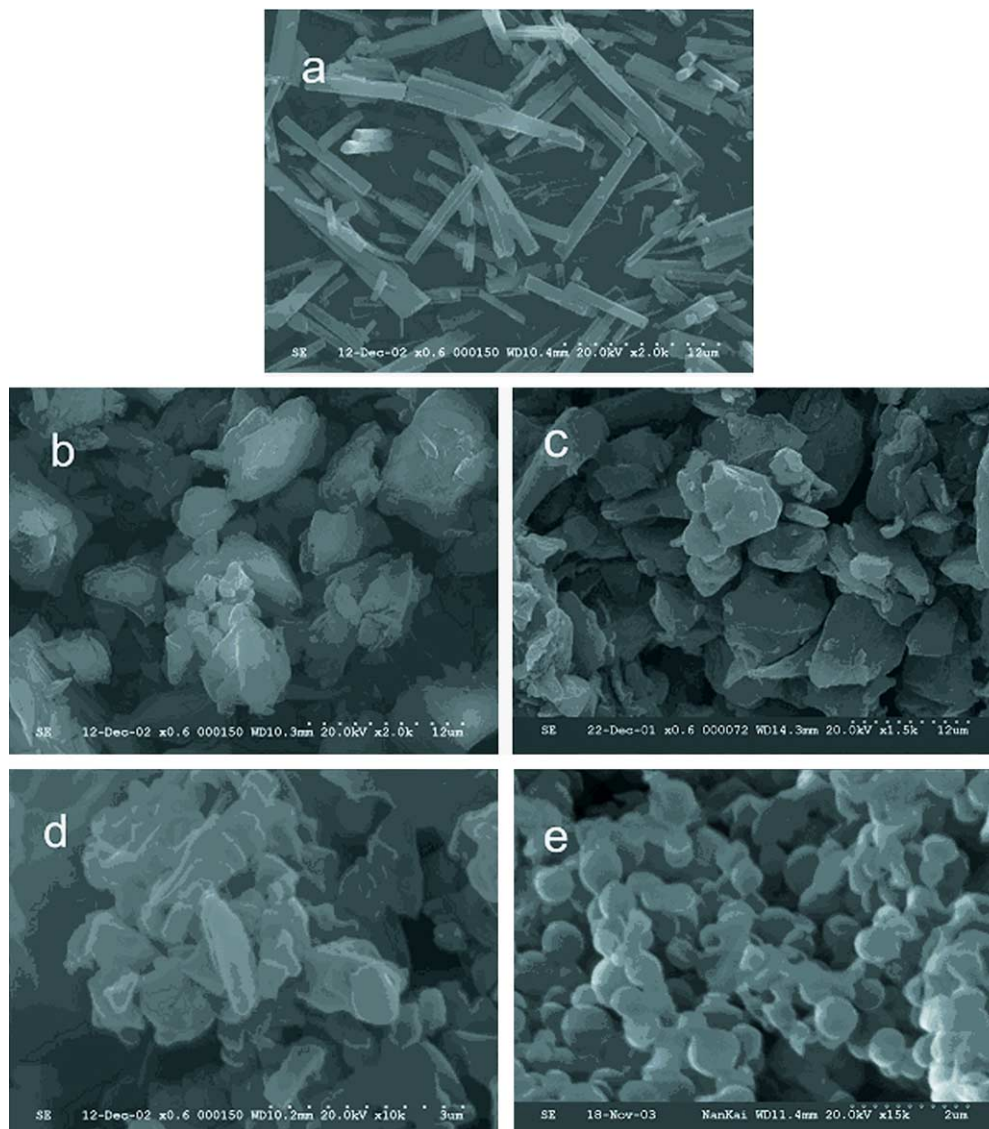

Figure 4. Possible binding mode of **1**/paclitaxel complex.

Figure 5. SEM images of (a) paclitaxel, (b) **1**, (c) **2**, (d) **1**/paclitaxel, and (e) **2**/paclitaxel complex.

drug and bis(β-CD)s. As can be seen in Figure 5, **1**/paclitaxel (or **2**/paclitaxel) complex can be characterized as a regular platelike morphology, the bis(β-CD) as a globular morphology, while the parent paclitaxel manifests a more sticklike morphology.

The powder X-ray diffraction patterns of paclitaxel, bis(β-CD), as well as their physical mixtures and inclusion complexes are illustrated in Figure 6. As can be seen in Figure 6, paclitaxel shows a diffractogram consistent with its crystalline nature (Fig. 6a), while bis(β-CD) **1** is amorphous (Fig. 6b). However, the physical mixture of paclitaxel with bis(β-CD) **1** (molar ratio 2:1) shows a diffractogram that can be characterized as a superimposition of crystalline paclitaxel and the amorphous bis(β-CD) (Fig. 6c). In contrast, **1**/paclitaxel complex (Fig. 6d) displays a different pattern especially in the 15°–25° (2θ) area where the peaks assigned to the paclitaxel almost disappear. In addition, the pattern of **1**/paclitaxel complex also exhibits the appreciable differences from that of the corresponding **1**/paclitaxel physical mixture in terms of not only the peak shape but also relative intensities in the 3°–8° (2θ) region, meaning that a new species, in this case **1**/paclitaxel complex, is formed between paclitaxel and bis(β-CD). The similar phenomena are also found in the case of **2**/paclitaxel system.

The FT-IR spectra of paclitaxel, bis(β-CD)s **1** and **2**, and their corresponding inclusion complexes are shown in Figure 7. The spectrum of paclitaxel shows strong absorption bands in the range of 1750–1600, 1300–1180, and 770–630 cm^{-1} (Fig. 7a). These characteristic bands all exist in the spectra of **1**/paclitaxel and **2**/paclitaxel complexes with negligible rightward shifts, which means the existence of paclitaxel in the complex. Moreover, the IR spectra of bis(β-CD)s **1** and **2** can be characterized by the intense bands at 3300–3500 cm^{-1} assigned to absorption by hydrogen-bonded OH groups as well as the bands at 2800–3000 cm^{-1} corresponding to vibration of the –CH and –CH$_2$ groups, which are equivalent to the bands of native β-CDs.[25] After association with paclitaxel, the spectra of the inclusion com-
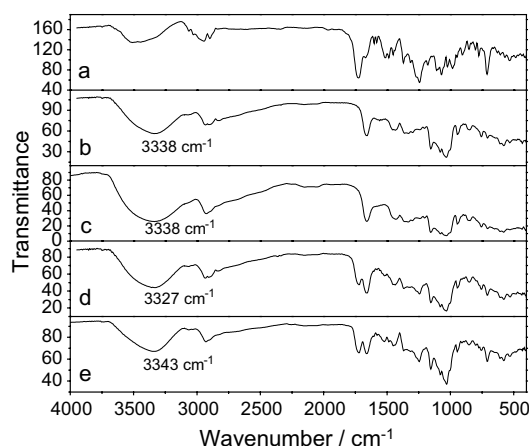

Figure 7. FT-IR spectra of (a) paclitaxel, (b) **1**, (c) **2**, (d) **1**/paclitaxel, and (e) **2**/paclitaxel complex in KBr tablet.

plexes show reduced intensities and certain shifts of the peak corresponding to hydrogen-bonded OH groups (for **1**/paclitaxel system from 3338 to 3327 cm^{-1}; for **2**/paclitaxel system from 3338 to 3343 cm^{-1}). In the control experiments, the spectra of the physical mixtures correspond simply to the superposition of the spectra of the individual components. These phenomena jointly suggest that after complex formation some of the existing hydrogen bonds formed between OH groups of CD are broken and thus provide an additional evidence for the formation of CD/paclitaxel complexes.

2.3. Thermal analysis of the complexes

The thermal properties of **1**/paclitaxel and **2**/paclitaxel complexes are investigated by thermogravimetric (TG) and differential thermal analysis (DTA) (Fig. 8). A systemic analysis on the TG and DTA curves shows that paclitaxel decomposes at 244 °C while parent bis(β-CD)s over 300 °C. Therefore, the peaks at about 228 and 238 °C in the DTA curves of **1**/paclitaxel and **2**/paclitaxel complexes should represent the temperature of the corresponding complex dissociating to its parent bis(β-CD) and paclitaxel, respectively. Furthermore,
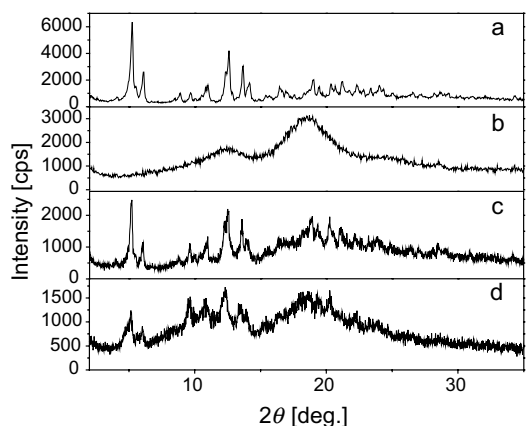

Figure 6. XRD patterns of (a) paclitaxel, (b) **1**, (c) physical mixture of **1** with paclitaxel (molar ratio 1:2), and (d) **1**/paclitaxel inclusion complex.
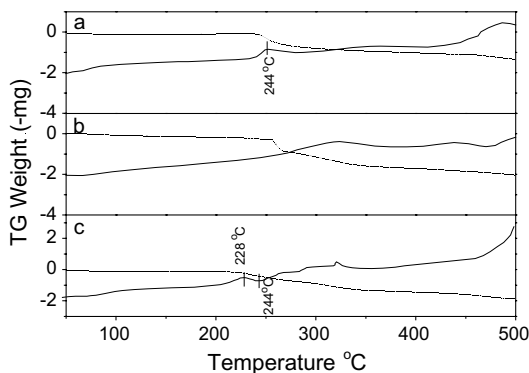

Figure 8. TG–DTA of (a) paclitaxel, (b) **1** and (c) **1**/paclitaxel, dotted curves represent TG, while solid ones DTA from room temperature to 500 °C.
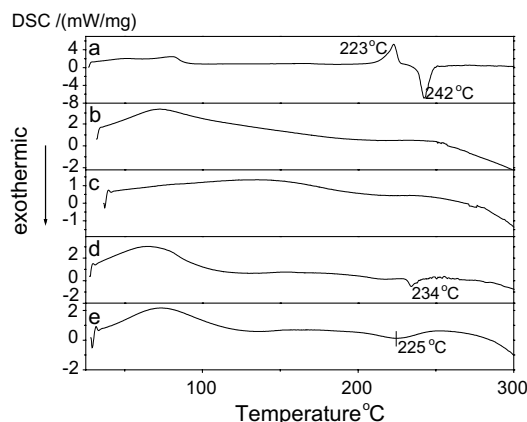
Figure 9. DSC curves of (a) paclitaxel, (b) **1**, (c) **2**, (d) **1**/paclitaxel, and (e) **2**/paclitaxel complex from room temperature to 300 °C.

differential scanning calorimetry (DSC) thermogram gives further information about the thermal property of **1**/paclitaxel and **2**/paclitaxel complexes (Fig. 9). The DSC curve of paclitaxel shows an endothermic peak at 223 °C and an exothermic peak at 242 °C. In contrast, the DSC curves of parent bis(β-CD)s do not show any peak in the region of 150–300 °C. However, we can find that, in the DSC curves of CD/paclitaxel complexes, the thermic peaks at 223 and 242 °C corresponding to free paclitaxel disappears, along with the appearance of a new exothermic peak at 234 °C (or 225 °C) in the case of **1**/paclitaxel (or **2**/paclitaxel) system, showing the **1**/paclitaxel complex is rather stable than **2**/paclitaxel complex. All these samples have been analyzed by HPLC confirming the thermal degradation occurrence. These results not only further confirm the formation of the CD/paclitaxel complexes, but also indicate that the resultant CD/paclitaxel complexes start to decompose only at a temperature above 200 °C, which means these complexes are fairly stable in thermal viewpoint.

2.4. Isothermal titration microcalorimetry (ITC) investigation of CD/paclitaxel complexes

To quantitatively assess the inclusion complexation behavior of paclitaxel with bis(β-CD)s, we perform the ITC experiments by gradually adding a solution of bis(β-CD) to the paclitaxel solution, due to the poor solubility of paclitaxel. In each run, a water–ethanol solution (1:1, v/v) of bis(β-CD)s (1.62 mM) in a 0.250 mL syringe has been sequentially injected with stirring at 300 rpm into the calorimeter sample cell containing a water–ethanol solution (1:1, v/v) of paclitaxel (0.164 mM). The sample cell volume is 1.4227 mL in all experiments. Each titration experiment is composed of 25 successive injections infections (10 μL per injection). Each titration of bis(β-CD) into the sample cell gives rise to a heat of reaction, caused by the formation of inclusion complexes between paclitaxel molecule and bis(β-CD). A control experiment has been performed to determine the heat of dilution by injecting a bis(β-CD) solution into a water–ethanol solution (1:1, v/v) containing no paclitaxel molecules. The dilution enthalpy is subtracted from the apparent enthalpy obtained

in each titration run, and the net reaction enthalpy is analyzed by using the 'sequential binding sites' model.

For this sequential binding, the binding constants K_1, K_2 must be defined relative to the progress of saturation, so that

$$K_1 = \frac{[MX]}{[M][X]} \quad K_2 = \frac{[MX_2]}{[MX][X]} \quad (1)$$

In the sequential model, there is no distinction as to *which* sites are saturated, but only as to the total number of sites that are saturated. If the sites are identical, then there is a statistical degeneracy associated with the sequential saturation since the first ligand to bind has more empty sites of the same kind to choose from than does the second ligand, etc. For identical interacting sites then, we can distinguish between the phenomenological binding constants K_i (defined by Eq. 1) and the intrinsic binding constants K_i^0 where the effect of degeneracies has been removed. The relationship between the two binding constants is given by

$$K_i = \frac{3-i}{i} K_i^0 \quad (2)$$

All calculations given below, as well as parameters reported from curve fitting, are in terms of K_1, K_2 values but the operator may convert to K_i^0 values, if desired, using Eq. 2. Since concentrations of all liganded species $[ML_i]$ can be easily expressed in terms of the concentration of the non-liganded species, $[M]$, then the fraction of total macromolecule having i bound ligands, F_i, are simply

$$F_0 = \frac{1}{P}$$

$$F_1 = \frac{K_1[X]}{P}$$

$$F_2 = \frac{K_1 K_2 [X]^2}{P} \quad (3)$$

where

$$P = 1 + K_1[X] + K_1 K_2 [X]^2$$

$$X_t = [X] + M_t \sum_{i=1}^{2} i F_i \quad (4)$$

Once n and values of fitting parameters K_1 and K_2 are assigned, then Eqs. 3 and 4 may be solved for $[X]$ by numerical methods (the Bisection method is used). After $[X]$ is known, all F_i may be calculated from Eq. 3 and the heat content after the ith injection is determined from

$$Q = M_t V_0 (F_1 \Delta H_1 + F_2 [\Delta H_1 + \Delta H_2]) \quad (5)$$

and, as before,

$$\Delta Q(i) = Q(i) + \frac{dV_i}{V_0} \left[\frac{Q(i) + Q(i-1)}{2} \right] - Q(i-1) \quad (6)$$

which then leads into the Marquardt minimization routine.

The ORIGIN software (Microcal), used for the calculation of the binding constant (K_1, K_2) and standard molar reaction enthalpy (ΔH_1, ΔH_2) from the titration curve, gives the relevant standard derivation on the basis of the scatter of data points in a single titration experiment. The potential surface of the five-dimensional fit (χ^2 as a function of four parameters K_1, ΔH_1; K_2, ΔH_2) is probably very 'flat' (if this word is applicable for description of a fifth-dimensional numerical universe), and therefore the scattering of the experimental data points does not allow the ORIGIN program to find an absolute minimum. We repeat computer simulations many times with various initial sets of the four parameters, using the constancy of χ^2 as a criterion of the results of calculations. Knowledge of the binding constant (Ks) and molar reaction enthalpy (ΔH^0) enable calculation of the standard free energy of binding (ΔG^0) and entropy changes (ΔS^0), according to the following equation:

$$\Delta G^0 = -RT \ln Ks = \Delta H^0 - T\Delta S^0$$

Therefore, this sequential two-step binding model is applied to generate an apparent binding constant ($K_1 \times K_2$) up to $2.04 \times 10^8 \, M^{-2}$ for the 2:1 **1**/paclitaxel inclusion complexation (Fig. 10). The derived thermodynamic parameters indicate that this inclusion complexation is a process cooperatively driven by enthalpy and entropy ($\Delta H_1^0 + \Delta H_2^0 = -10.2 \, \text{kJ/mol}$, $T\Delta S_1^0 + T\Delta S_2^0 = 37.3 \, \text{kJ/mol}$), suggesting that the van der Waals forces, hydrophobic interactions, and desolvation effect jointly contribute to the overall inclusion process. This is contrast to the thermodynamics of binding for simple cyclodextrin hosts and their molecular guests in that these associations tend to be enthalpically driven.[26] Unfortunately, we fail to obtain the stability constant and thermodynamic parameters for **2**/paclitaxel system, since the heat of the inclusion process is too small to ca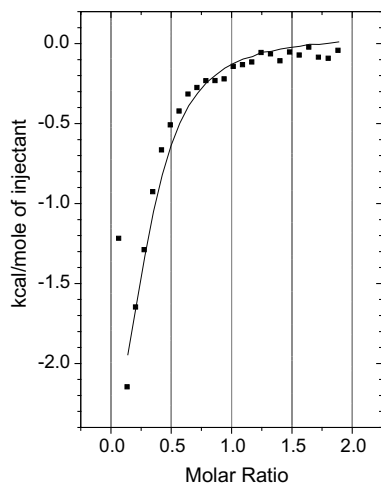lculate the corresponding thermodynamic parameters. This phenomenon may indicate the binding affinity of **2**/paclitaxel system is far weaker than that of **1**/paclitaxel system.

2.5. Solubility of the complexes

The water solubility of CD/paclitaxel complex is assessed by the preparation of its saturated solution.[13c] Excess amount of complex is put into 5 mL of water (ca. pH 6.0) and the mixture is stirred for 1 h. After removing the insoluble substance by filtration, the filtrate is evaporated under reduced pressure to dryness and the residue is dosed by weighing method. The results show that the water solubility of **1**/paclitaxel and **2**/paclitaxel complexes, comparing with that of paclitaxel (30 μg/mL;[23a] 0.7 μg/mL;[23b] 6 μg/mL[23c]), is dramatically increased to approximately 2.0 and 0.9 mg/mL (calculated as paclitaxel residue), respectively. In the control experiment, clear solution is obtained after dissolving **1**/paclitaxel (4.8 mg) or **2**/paclitaxel (3.3 mg) complex, which is equivalent to 2.0 or 0.9 mg of paclitaxel, in 1 mL of water at room temperature. This subsequently confirms the reliability of the obtained satisfactory water solubility of CD/paclitaxel complexes.

2.6. Biological activity

The cytotoxicity tests for **1**/paclitaxel and **2**/paclitaxel complexes have been evaluated in vitro for antiproliferative activity against human K562 erythroleukemia cell line by the MTT cytotoxicity assay using parent bis(β-CD)s **1** and **2** and free paclitaxel as reference compounds. The IC$_{50}$ values that represent the concentration of a drug required for 50% reduction of cellular growth have been calculated. As expected, no antiproliferative activity of bis(β-CD)s **1** and **2** can be observed in the concentration range of 1.0×10^{-7}–1.0×10^{-11} mol/dm^3. Excitingly, **1**/paclitaxel complex presents a satisfactory antiproliferative activity; its IC$_{50}$ value (calculated as paclitaxel residue) is 6.0×10^{-10} mol/dm^3, which is even lower than that of free paclitaxel (9.8×10^{-10} mol/dm^3).

Figure 10. Heat effects of complexation of paclitaxel with bis(β-CD) **1** for each injection during titration microcalorimetric experiment in a water–ethanol solution (1:1, v/v) at 25 °C.
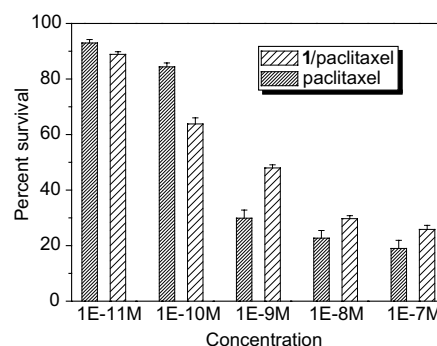

Figure 11. Antiproliferative activity of **1**/paclitaxel complex and paclitaxel. Each experiment consisted of four wells per concentration. The percent survival plotted is the average of all 12 wells of the three separate assays. Error bars represent standard deviation. The graphs are generated using Origin. The concentrations mentioned in this figure refer to the molar concentration of free paclitaxel and **1**/paclitaxel complex, respectively.

On the other hand, **2**/paclitaxel complex, due to its lower paclitaxel content and weaker CD/drug association than those of **1**/paclitaxel, gives a disappointing inhibitive ability lower than 10% for K562 erythroleukemia after 72 h.

In addition, the antiproliferative activities of **1**/paclitaxel complex and free paclitaxel against human K562 erythroleukemia cell line at different concentrations are shown in Figure 11. From this figure, we can deduce that the concentration dependence of the in vitro cell antiproliferative activity of **1**/paclitaxel complex is somewhat different from that of free paclitaxel. Free paclitaxel exhibits a very effective antiproliferative activity against K562 erythroleukemia at a concentration higher than 1×10^{-9} mol/dm^3. However, when further diluting the paclitaxel solution to 1×10^{-10} mol/dm^3 or lower, its activity decreases sharply. In contrast, the antiproliferative activity of **1**/paclitaxel complex displays a smooth decline when its concentration decreases from 1×10^{-7} to 1×10^{-11} mol/dm^3, which will be potentially useful to its clinical application.

3. Experimental section

3.1. General

NMR experiments were performed on a Varian Mercury VX300 spectrometer (300 MHz) at 298 K in a deuterium oxide solution. Tetramethylsilane was used as reference and no correction was made for susceptibility of the capillary. NOESY spectrum was performed in D$_2$O (300 MHz) with a mixing time of 400 ms. SEM images were recorded on a HITACHI S-3500N Scanning Electron Microscope. Thermogravimetric (TG) and differential thermal analysis (DTA) were recorded with a RIGAKU Standard type. Samples were heated at 10 °C/min from room temperature to 500 °C in a dynamic nitrogen atmosphere (flow rate = 70 mL/min). Powder X-ray patterns were obtained using a Rigaku D/max-2500 diffractometer with Cu Kα radiation (40 kV, 100 mA). Powder samples were mounted on a sample holder and scanned with a step size of 2 = 0.02° between $2\theta = 3°$ and 35°. FT-IR spectra were obtained on a Bio-Rad FTS 135 FT-IR spectroscopy device. The samples were mixed with KBr and compressed as disks; 16 scans were signal averaged at a resolution of 8 cm^{-1}. Differential scanning calorimetry (DSC) was performed with a NETZSCH DSC 204 instrument with a heating rate of 10 °C/min from 26 to 300 °C with a heating rate of 10 K/min. ITC was performed on an isothermal calorimeter at 25 °C, using ethanol–water (1:1, v/v) as solvent. Tetraethylenepentaamino-bridged bis(β-CD) (**1**), triethylenetetraamino-bridged bis(β-CD) (**2**), ethylenediamino-bridged bis(β-CD) (**3**), and **1**/Cu(II) complex (**4**) are synthesized according to the reported procedures, respectively.[27,28] Molecular model study was performed with the CAChe 3.2 program (Oxford Molecular Co., 1999). The initial geometry of β-CD used in this study was taken from the crystal structure described in the literature,[29] and the energy of this structure was minimized using the MM2 force field.

3.2. Preparation of the 1/paclitaxel complex[30]

To generate drug–cyclodextrin complexes, paclitaxel (0.03 mM) and **1** (0.01 mM) were completely dissolved in a mixed solution of ethanol and water (v:v = 1:5) and stirred for 3 days at room temperature. After evaporating the ethanol from the mixed solution, the uncomplexed paclitaxel was removed by filtration. The filtrate was again evaporated to remove water and dried in vacuum to give **1**/paclitaxel complex (38.5 mg, yield 93%).[1] H NMR (300 MHz, D$_2$O, TMS): δ 0.78–1.88 (m, 26H, paclitaxel protons), 1.88–3.04 (m, 38H, NHCH$_2$ of **1** and paclitaxel protons), 3.04–4.11 (m, 84H, H-2–6 of **1**), 4.78–5.04 (s, 14H, H-1 of **1**), 7.08–8.10 (m, 30H, ArH of paclitaxel).

3.3. Preparation of complex 2/paclitaxel

Complex **2**/paclitaxel was prepared in ca. 85% yield from bis(β-CD) **2** and paclitaxel. ^{1}H NMR (300 MHz, D$_2$O, TMS): δ 0.78–1.88 (m, 13H, paclitaxel protons), 1.88–3.04 (m, 31H, NHCH$_2$ of **2** and paclitaxel protons), 3.04–4.11 (m, 84H, H-2–6 of **2**), 4.78–5.04 (s, 14H, H-1 of **2**), 7.08–8.10 (m, 15H, ArH of paclitaxel).

3.4. Cell and treatments

Cells were cultured at 5×10^5/mL in RPMI 1640 supplemented with 10% heat-inactivated fetal bovine serum at 37 °C in a humidified atmosphere of 5% CO$_2$ in air. Cells were seeded at 5×10^4/mL and treated with the indicated amounts of the complex.

3.5. Measurement of cytotoxicity

The effect of the complex was evaluated as cell survival after treatment. Cell viability was evaluated by a microculture tetrazolium reduction assay using MTT (3-(4,5-dimethyltriazol-2-yl) 2,5-diphenyltetrazolium bromide; Sigma). Briefly, 50 mL of MTT stock solution (2 mg/mL in PBS) was added to 150 mL cell cultures in 96-microwell flat-bottom plates for 4 h incubation at 37 °C. Plates were then centrifuged and MTT-containing culture medium removed. Precipitated formazan was dissolved in 150 mL DMSO. Results were read with 15 min in a spectrometer at 577 nm, and the means of triplicates were calculated. Cell inhibition rate is expressed as percentage of control samples.

References and notes

1. Wani, M. C.; Taylor, H. L.; Wall, M. E.; Coggon, P.; McPhail, A. T. *J. Am. Chem. Soc.* **1971**, *93*, 2325.
2. Cragg, G. M. *Med. Res. Rev.* **1998**, *18*, 315.
3. Manfredi, J. J.; Horwitz, S. B. *Pharmacol. Ther.* **1984**, *25*, 83.

4. Safavy, A.; Bonner, J. A.; Waksal, H. W.; Buchsbaum, D. J.; Yancey Gillespie, G.; Khazaeli, M. B.; Arani, R.; Chen, D.-T.; Carpenter, M.; Raisch, K. P. *Bioconjugate Chem.* **2003**, *14*, 302.

5. Wrasidlo, W.; Gaedicke, G.; Guy, R. K.; Renaud, J.; Pitsinos, E.; Nicolaou, K. C.; Reisfeld, R. A.; Lode, H. N. *Bioconjugate Chem.* **2002**, *13*, 1093.

6. Schmidt, F.; Ungureanu, I.; Duval, R.; Pompon, A.; Monneret, C. *Eur. J. Org. Chem.* **2001**, *11*, 2129.

7. Altstadt, T. J.; Fairchild, C. G.; Golik, J.; Johnston, K. A.; Kadow, J. F.; Lee, F. Y.; Long, B. H.; Rose, W. C.; Vyas, D. M.; Wong, H.; Wu, M.-J.; Wittman, M. D. *J. Med. Chem.* **2001**, *44*, 4577.

8. Niethammer, A.; Gaedicke, G.; Lode, H. N.; Wrasidlo, W. *Bioconjugate Chem.* **2001**, *12*, 414.

9. Davignon, J. P.; Cradock, J. C. In *Principles of Chemotherapy*; Carter, S. K., Hellman, K., Eds.; McGraw-Hill: New York, 1987.

10. Saenger, W. *Angew. Chem., Int. Ed. Engl.* **1980**, *19*, 344.

11. Wenz, G. *Angew. Chem., Int. Ed. Engl.* **1994**, *33*, 803.

12. Szejtli, J. *Chem. Rev.* **1998**, *98*, 1743.

13. (a) Stella, V. J.; Rajewaki, R. A. *Pharm. Res.* **1997**, *14*, 556; (b) Park, C. W.; Kim, S. J.; Park, S. J.; Kim, J. H.; Kim, J. K.; Park, G. B.; Kim, J. O.; Ha, Y. L. *J. Argic. Food Chem.* **2002**, *50*, 2977; (c) Montassier, P.; Duchêne, D.; Poelman, M.-C. *Int. J. Pharm.* **1997**, *153*, 199; (d) Arias-Blanco, M. J.; Moyano, J. R.; Perez-Martinez, J. I.; Gines, J. M. *J. Pharm. Biomed. Anal.* **1998**, *18*, 275.

14. Bodor, S. N. U.S. Patent, 5024998, 1991.

15. Adam, J. M.; Jonathan Bennett, D.; Born, A.; Clark, J. K.; Feilden, H.; Hutchinson, E. J.; Palin, R.; Prosser, A.; Rees, D. C.; Rosair, G. M.; Stevenson, D.; Tarver, G. J.; Zhang, M.-Q. *J. Med. Chem.* **2002**, *45*, 1806.

16. Baussanne, I.; Benito, J. M.; Mellet, C. O.; Fernandez, J. M. G.; Defaye, J. *ChemBioChem* **2001**, *2*, 777.

17. Ren, X. J.; Xue, Y.; Liu, J. Q.; Zhang, K.; Zheng, J.; Luo, G.; Guo, C. H.; Mu, Y.; Shen, J. C. *ChemBioChem* **2002**, *3*, 356.

18. Sharma, U. S.; Balasubramanian, S. V.; Straubinger, R. M. *J. Pharm. Sci.* **1995**, *84*, 1223.

19. (a) von Bommel, K. J. C.; de Jong, M. R.; Metselaar, G. A.; Verboom, W.; Huskens, J.; Hulst, R.; Kooijman, H.; Spek, A. L.; Reinhoudt, D. N. *Chem. Eur. J.* **2001**, *7*, 3603; (b) de Jong, M. R.; Engbersen, J. F. J.; Huskens, J.; Reinhoudt, D. N. *Chem. Eur. J.* **2000**, *6*, 4034; (c) Michels, J. J.; Huskens, J.; Reinhoudt, D. N. *J. Am. Chem. Soc.* **2004**, *124*, 2056.

20. (a) Nelissen, H. F. M.; Kercher, M.; de Cola, L.; Feiters, M. C.; Nolte, R. J. M. *Chem. Eur. J.* **2002**, *8*, 5407; (b) Venema, F.; Nelissen, H. F. M.; Berthault, P.; Birlirakis, N.; Rowan, A. E.; Feiters, M. C.; Nolte, R. J. M. *Chem. Eur. J.* **1998**, *4*, 2237.

21. Baugh, S. D. P.; Yang, Z.; Leung, D. K.; Wilson, D. M.; Breslow, R. *J. Am. Chem. Soc.* **2001**, *123*, 12488.

22. Moser, J. G.; Rose, I.; Wagner, B.; Wieneke, T.; Vervoorts, A. *J. Inclusion Phenom. Mol. Recognit.* **2001**, *39*, 13.

23. (a) Swindell, C. S.; Krauss, N. E.; Horwitz, S. B.; Ringel, I. *J. Med. Chem.* **1991**, *34*, 1176; (b) Mathew, A. E.; Mejillano, M. R.; Nath, J. P.; Himes, R. H.; Stella, V. J. *J. Med. Chem.* **1992**, *35*, 145; (c) Tarr, B. D.; Yalkowsky, S. H. *J. Parenteral Sci. Technol.* **1987**, *41*, 31.

24. Lorenz, S. A.; Bigwarfe, J. R. P. M.; Balasubramanian, S. V.; Fetterly, G. J.; Straubinger, R. M.; Wood, T. D. *J. Pharm. Sci.* **2002**, *91*, 2057.

25. Perdomo-López, I.; Rodrǐguez-Pérez, A. I.; Yzquierdo-Peiró, J. M.; White, A.; Estrada, E. G.; Villa, T. G.; Torres-Labandeira, J. J. *J. Pharm. Sci.* **2002**, *91*, 2408.

26. Loftsson, T. *J. Pharm. Sci.* **1996**, *85*, 1017.

27. Liu, Y.; You, C.-C.; Li, B. *Chem. Eur. J.* **2001**, *7*, 1281.

28. Tabushi, I.; Kuroda, Y.; Shimokawa, K. *J. Am. Chem. Soc.* **1979**, *101*, 1614.

29. Betzel, C.; Saenger, W.; Hingerty, B. E.; Brown, G. M. *J. Am. Chem. Soc.* **1984**, *106*, 7545.

30. Liu, Y.; Chen, G.-S.; Li, L.; Zhang, H.-Y.; Cao, D.-X.; Yuan, Y.-J. *J. Med. Chem.* **2003**, *46*, 4634.